AJBAR Vol 1(5), 2022: 103-125, ISSN: 2811-2881

Arid Zone Journal of Basic and Applied Research

Faculty of Science, Borno State University
Maiduguri, Nigeria

Journal homepage: https://www.azjournalbar.com

Research Article

Adsorption of Cr (VI) ion from Aqueous Solution Using Unmodified Desert Date Peels (*Balanites aegyptiaca*) Composite with MWCNTs: Isotherm and Kinetic Studies

[1]*Alkali, M.I., [2]Abdus-Salam, N., [2]Bello, M.O., [3]Musa, M.O., [4]Jimoh, A.A., [5]Dikwa, M.K. and [6]Abdullahi, M.M.

[1]Department of Chemistry, Borno State University, Maiduguri-Nigeria
[2]Department of Chemistry, University of Ilorin, Nigeria
[3]Department of Chemistry, Al-Hikima University, Nigeria
[4]Department of Chemistry, Kwara State University, Malete-Nigeria
[5]Department of Chemistry, University of Maiduguri, Nigeria
[6]Nigerian Natural Medicine Development Agency
*Corresponding author: ibrambnanabe@gmail.com, doi.org/10.55639/607zyxts

ARTICLE INFO:

Keywords:
Unmodified Desert Date Peels,
Modified Desert Date Composite,
Chromium (VI) ions,
Langmuir

ABSTRACT

Continuous Changing of human lifestyles has consistently added different notorious anthropogenic pollutants into aquatic matrices. Exterminating these toxic pollutants is feasible using adsorption studies instead of the traditional water purification methods. The purpose of this study was to investigate the adsorption of Cr (VI) ion from aqueous using Unmodified Desert Date (UDD) Peels as a low-cost adsorbent and composite with multi-walled carbon nanotubes (UDDC). A batch adsorption experiment was conducted to evaluate the maximum quantity adsorbed of Cr (VI) ions from an aqueous medium under various conditions. The Fourier-Transform Infrared Spectroscopy (FTIR) revealed 3448.84 cm^{-1} and 3441.12 cm^{-1} which corresponds to O-H stretching vibration modes for UDD and UDDC and 1620.26 cm^{-1} relates to C=O stretching vibrations for both UDD and UDDC respectively. The maximum adsorption capacity (q^e) is found to be 114.11 and 741.14 (mg/g) for UDD and UDDC respectively. The results showed that UDDC has a large adsorption capacity due to its higher surface area. The adsorption data were fitted well into Langmuir with correlation coefficient (R^2) values close to unity 0.9076 and 0.9069 for UDD and UDDC respectively. Kinetic studies showed a good correlation coefficient pseudo-second-order kinetic model fitted very well into UDD and UDDC with (R^2) values 0.9173 and 0.9943 respectively. The results indicated that UDDC could be used as a potential adsorbent for the adsorption of Cr (VI) ions from an aqueous solution

Corresponding author: Alkali, M.I, Email: ibrambnanabe@gmail.com
Department of Chemistry, Borno State University, Maiduguri-Nigeria

INTRODUCTION

Nowadays, the demand for activated carbons in Nigeria is getting serious attention like other developing nations. The importation of synthesized adsorbents at a very high cost and considering the high rate of Covid-19 cases in the developed nations, whereas a vast number of agricultural wastes littering the environment which in turn could be used for the treatment of wastewater. If locally sourced technology is developed, it will eventually create wealth from the waste and reduce over dependent on importation by converting these available adsorbents into activated carbons in the new normal environment (Abdus-Salam and Buhari, 2016).

In the rapidly improving field of nanotechnology, nanomaterials are on the front line. Their special property most especially the surface area gives them an edge over other materials. This improves their applications in various human activities (Sweetman *et al*., 2017; Farghali *et al*., 2012). Multi-walled carbon nanotubes (MWCNTs) have been identified as peculiar inorganic nanomaterial due to their superior properties with functional versatility leading to unending interest among scientific researchers (Dada *et al*., 2018). To date, much effort has been devoted to preparing and synthesizing various composites based on carbon nanotubes (CNTs) with activated carbons (Li *et al*., 2006). Composite materials based on activated carbons and inorganic MWCNTs integrate the unique characteristics and functions of the two types of components and may also exhibit some new properties caused by combinatory effects between the two kinds of materials (Peng *et al*., 2009). Therefore, these composite materials have shown very attractive potential applications in the scientific environment.

Chromium is one of the toxic metals that have been studied because it can be formed in both cationic and anionic water. Chromium exists in oxidation states +2, +3, +4, +5 and +6, but the most common, stable and abundant forms are chromium (III) and chromium (VI) (ATSDR, 1998). Chromium (III) exists in the form of a cation, Cr^{3+} and it occurs naturally in the environment while chromium (VI) exists in the anionic form (chromate) produced by the industrial process for laboratory reagents and manufacturing intermediates (Gomez and Callao, 2006; Aneyo *et al*. 2016). The permissible level of Cr (VI) in drinking and wastewater are 0.1 mg/L and 0.05 mg/L respectively (WHO, 2011; Ayeni, 2014). Cr (VI) ion affects almost every vital organ and system in the body. Exposure to high Cr (VI) can severely damage the brain and kidneys in adults or children and eventually causes death (Kinuthia *et al*., 2020). Hence, the removal of Cr (VI) ion from wastewater is paramount to protect public health in the analytical environment.

Several methods such as chemical precipitation (Eltayeb and Khan, 2019), ion exchange (Khan *et al*., 2018), reverse osmosis (Duan *et al*., 2018), electrochemical reduction (Khan *et al*., 2019), filtration and adsorption (Çalımlı *et al*., 2019) and membrane separation (Khan and Khan, 2010) have been developing to remove Cr (VI) ion from wastewater. However, these methods are either expensive for wastewater treatment and disposal of secondary sludge when Cr (VI) ion in wastewater is at a low concentration (Labied *et al*., 2018). In contrast, the adsorption method is one of the cheapest and preferred methods because of the abundance of agricultural waste in the environment (Giwa *et al*., 2019). Therefore, there is a need for a constant and regular search for alternative low-cost adsorbents.

There are different types of adsorbents that are in abundance and inexpensive in the

environment. However, many scientific researchers have worked on various adsorbents in the treatment of wastewater as well as carbon nanotubes with examples by Danmallam *et al*. (2020) neem seed husk; Gebretsadik *et al*. (2020) Eucalyptus camaldulesis; Fan *et al*. (2019) Rice straw; Adebayo *et al*. (2020) Goethite activated carbon; Ahmed *et al*. (2017) carbon nanotubes; Dargahi *et al*. (2016) Magnesium Oxide Nanoparticles; Dehgani *et al*. (2015) single walled and multi-walled carbon nanotubes; Yang *et al*. (2015) Longan seed; Krishna-Kumar *et al*. (2015) functionalized multi-walled carbon nanotube; Adegoke *et al*. (2014) hematite (alpha-Fe_2O_3) nanoparticles; Moosa *et al*. (2014) carbon nanotubes; Deveci and Kar (2013) Bio Char; Bansal *et al*. (2009) agricultural waste; El-Shafey (2005) modified rice husk; Bishnoi *et al*. (2004) activated rice husk etc. have successfully used these adsorbents for the adsorption of Cr (VI) ion from aqueous medium.

The present research aims to prepare Desert Date peels from agricultural waste and composite with multi-walled carbon nanotubes (MWCNTs) for adsorption of Cr (VI) ion. The objectives are to characterize the morphology and the surface functional groups of the adsorbents using a Scanning electron microscope (SEM) and Fourier transmission infrared (FTIR). The effects of batch experiment parameters such as initial concentration, adsorbent dosage, contact time, pH and temperature were determined to establish optimum conditions for the adsorption process. Also, various isotherm and kinetic models have been studied for their usefulness in correlating the experimental data.

MATERIALS AND METHODS

Sample Collection and Preparation

The Desert date peels (*Balanite aegyptica*) were harvested from the plant within Mobbar Local Government Area of Borno State, North Eastern region of Nigeria that is located between latitude 13.1330˚ N and longitude 12.7135˚E and transported to the laboratory for preliminary treatment before use. The sample was washed thoroughly with tap water, followed by washing with deionized water and finally dried in an oven for 24 hours at 120 °C. After that, the Unmodified Desert Date peels (UDD) were crushed to fine powder by a mortar and pestle stable arm grinder and sieved with 0.01 mm. The fine powder sample was carbonized at 400 ^oC for 1 hr in a pyrolyser and subsequently used for the adsorption studies.

Reagents and Instruments

All chemicals used are analytical-grade reagents. Multi-walled carbon nanotubes with an average diameter between 50 and 90 nm (95 %), Potassium dichromate $K_2Cr_2O_7$ (99.5 %), KOH (95 %), H_2SO_4 (97 %), HNO_3 (65 %) were purchased from Sigma-Aldrich, Iran.

Batch Adsorption Experiment

The equilibrium adsorption of the Cr (VI) ion unto Unmodified Desert Date (UDD) and Unmodified Desert Date Composite (UDDC) are carried out by contacting 0.01g of the adsorbents with 20 mL of different concentrations from 400 mg/L–1200 mg/L in 250 cm^3 pyrex conical flask, shaken in water bath shaker at 25 ^oC intermittently for 5 hrs at 230 rpm to remove the residual aqueous concentration. The initial and final concentrations of the mixtures are filtered, and the residual concentration of the filtrate was analyzed using UV – a visible Spectrophotometer at λ max (510 nm). The amount of equilibrium qe adsorbed (mg/g) of Cr (VI) ion was calculated using the formula reported by (Nwosu *et al*., 2017).

$$q_e = \frac{v(c_i - c_e)}{M} \quad (1)$$

Where qe = is the amount of Cr (VI) ion adsorbed from the solution in (mg/g) at

equilibrium, Ci = the concentration before adsorption (mg/L), Ce = the concentration after adsorption (mg/L), V = volume of the adsorbate (L), and M = is the weight in a gram of the adsorbent (g) respectively (Abdus-Salam and Bello, 2015). The extent of adsorption was calculated using equation (2)

$$\% \text{ Adsorption } = \frac{c_i - c_e}{c_i} \times \frac{100}{1} \qquad (2)$$

Preparation of MWCNTs Composite

A slightly modified procedure by Yudianti *et al*. (2011); Kim *et al*. (2017) was adopted for the epoxidation of the MWCNTs. Two different chemicals are used for the epoxidation processes (400 ml, 60 % HNO_3 and 400 ml, 60 % H_2SO_4 acid concentrations) to achieve reasonable surface oxidation of the carbon tubes. The epoxidated MWCNTs were composited with the Unmodified Desert Date (*Balanite aegyptica*) peels at 1:2 (w/w) according to a modified procedure adopted by Farghali *et al*. (2017). The pre-weighed epoxidated MWCNTs were poured into 100 ml absolute ethanol and stirred thoroughly at 80 ^oC for 6 hr under reflux with 2 g each of the Unmodified Desert Date peels. Thereafter, the prepared composite was filtered and finally dried in an oven at 105 ^oC for 2 hr. The dried composited sample was characterized and used for an adsorption study.

Characterization of the adsorbents

The characterization of the adsorbents was carried out using Scanning Electron Microscope (SEM) coupled with Energy Dispersive X-ray (EDX) and Fourier Transmission Infra-red (FTIR) spectroscopy. The SEM is a characterization analysis usually used to determine the morphology, shape and particle size of an adsorbent (Abdus-Salam and Ikudisiyi, 2017). SEM analysis was carried out in the Department of Chemistry, University of Cape Town, Rondebosch, South Africa. The results were obtained from the analysis at 10.00 kx magnification of Tescan MIRA 3 SEM. However, the FTIR is an essential tool to determine the surface functional groups and bond formation of the adsorbents Boudaoud *et al*. (2017) and it was carried out in the Department of Chemistry, Redeemer's University, Osun, Nigeria. The sample spectra were recorded over the range of 400 – 4000 cm^{-1}.

RESULTS AND DISCUSSION

Characterization Analysis

Scanning Electron Microscopy (SEM)

The SEM micrograph of UDD peels and UDDC are presented in Figures 3a & b respectively. It can be observed that UDD peels showed lamellar stratified surface, cavities and pores on the activated carbon sample with several large clusters of mesopores spotted on it which revealed that it is highly porous. Similarly, UDDC revealed sparsely web shaped pores on the surface of the carbon nanotubes which look similar to the reported literature of (Azeeze and Adekola, 2016).

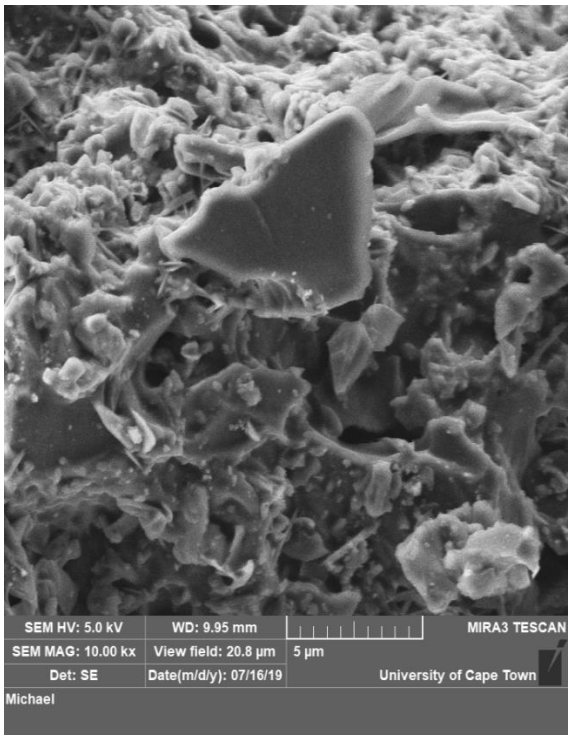

Figure 1a: SEM Micrograph of UDD Peels

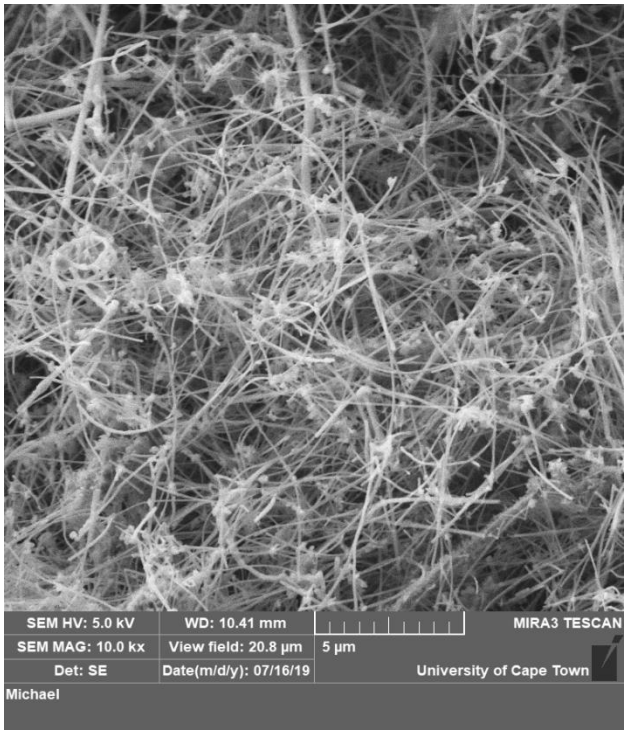

Figure 1b: SEM Micrograph of UDDC

Fourier Transform Infrared Spectra (FTIR)

The UDD peels and UDDC spectra are presented in Figures 2a & b respectively. The broadband peak of UDD at 3448.84 cm-1 corresponds to the O-H stretching mode of hydroxyl groups of unmodified activated carbon. Another interesting band at 1620.26 cm-1 which be related to the C=O carboxyl group (Vukovic and Marinkovic, 2011). Similar results have been reported by Giwa *et al*. (2019) on a desert date seed shell activated carbon cited somewhere. However, in the FT-IR spectrum of UDDC, the peaks at 3441.12 and 1620.26 cm-1 can be attributed to the stretching vibrations of O-H and C=O of carboxyl groups respectively. In addition, the peak at 1384.94 cm-1 is assigned to the CH3 bending vibration. The presence of this peak suggests that the oxidation of the MWCNTs is reflected on the composite. The results obtained were in line with the Preparation, characterization and adsorption performance of the KOH-activated carbons derived from kenaf fibre for lead (II) removal from wastewater of (Chowdhury *et al*., 2011).

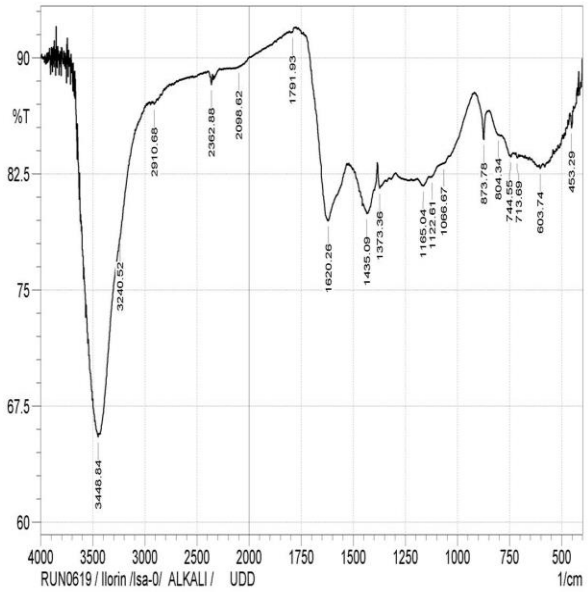

Figure 2a: FT-IR spectrum of UDD Peel

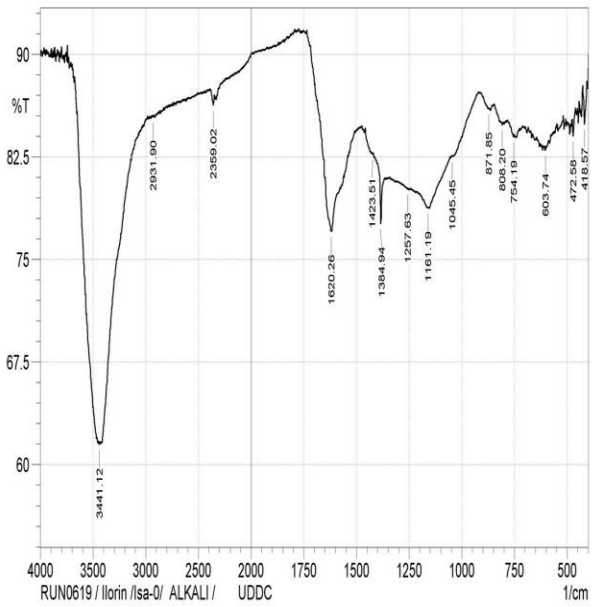

Figure 3b: FT-IR spectrum of UDDC

Batch Adsorption Experiment

Effect of the Initial Metal Ions Concentration

The effect of initial metal ion concentration on UDD and UDDC adsorption ability is presented in Figure 3. The effect of initial metal ion concentration on the adsorption ability of UDD and UDDC was determined by varying their concentrations; 1200-400 mg/L. The maximum quantity adsorbed for Cr (VI) ion onto UDD and UDDC is 114.11 and 741.14 (mg/g) at 1000 and 400 (mg/L) of adsorbate concentration. It was observed that the maximum quantity adsorbed per gram (qe) for UDD increased with increasing initial adsorbate concentration due to the high availability of Cr (VI) ion in solution, whereas qe of UDDC was obtained at the initial stage of adsorbate concentration. Similar trends have been reported by Buhari *et al*. (2020); Yunusa and Ibrahim, (2019). However, the maximum quantity adsorbed of the UDDC at the initial adsorbate concentration of the composite could be attributed to the strength of the functionalized MWCNTs coupled with the composite material (Farghali *et al.*, 2017). It is generally accepted that the mechanism for the adsorbed metal ion is related to the surface properties of activated carbons due to the saturation of active sites on the adsorbent (Adegoke *et al*., 2016; Habte *et al*., 2020).

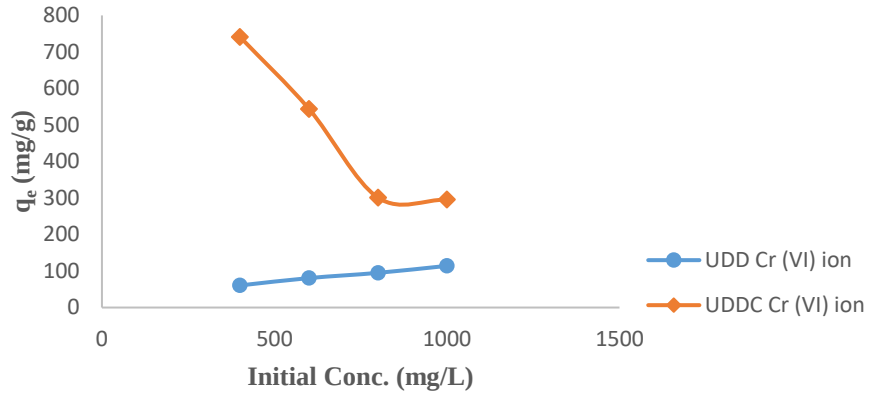

Figure 3: Effect of Initial Conc. for Cr (VI) ion onto UDD Peels & UDDC

Table 1: Comparison of q_e (mg/g) of UDD and UDDC with other adsorbents for Cr (VI) ion uptake

Adsorbents	**q_e (mg/g)**	**Authors**
MWCNTs	250	Moosa *et al*., 2015
Rice Starw	97.12	Lee *et al.*, 2017
Coffee pulp	13.48	Aguilar *et al.*, 2019
Ade 1	5.03	Adegoke *et al.*, 2014
UDD	114.11	This Study
UDDC	741.14	This Study

Effect of Adsorbent Dosage

To determine the minimum possible dosage for the maximum adsorption of metal ion, the amount of adsorbent dosage was varied, 0.01 g, 0.02 g, 0.03 g and 0.05 g in 100 mL of 20 mg/L metal ion solution onto UDD and UDDC respectively. These experiments were conducted under optimized pH conditions for each of the sample. Figure 4 illustrates the effect of variation dosage on the adsorption Cr (VI) ion. However, the maximum quantity adsorbed (q_e) was obtained at the lower dosage 0.01 g for both adsorbents. This could be related to inaccessibility of the active sites or due to overlapping of the adsorption sites with higher adsorbent dosage (Alghamdi *et al*., 2019). This observation suggests that adsorption is almost directly proportional to the amount of the dosage. A similar result was also obtained from the research cited by (Zhang *et al*., 2008).

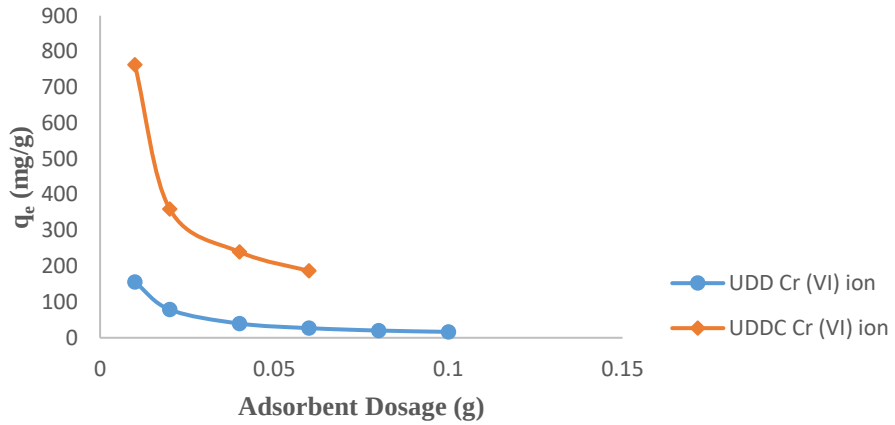

Figure 4: Effect of Adsorbent Dosage for Cr (VI) ion onto UDD Peels & UDDC

Effect of Contact Time

The effect of contact time helps to understand the rate of reaction and the time the adsorption process reaches the equilibrium state (Ugbe *et al*., 2017). The effect of contact time on the adsorption of Cr (VI) ion was investigated at different time intervals in the range of 10-90 min and the results are presented in Figure 5 onto UDD and UDDC respectively. The maximum quantity adsorbed of UDD was achieved within 30 min whereas the optimum contact time for the UDDC was achieved at 60 min. This could be attributed to the available number of active sites on the surface of carbons which became saturated at the later stages of contact time due to the decreased number of active sites (Adebayo *et al*., 2014). Similar behaviour was observed in malachite green adsorption prepared with desert date shell reported by (Yunusa *et al*., 2020). However, in the case of composite, the maximum quantity adsorbed was noticed within 60 min, which took a relatively longer time to attain equilibrium due to the higher amount of adsorbate molecules that will diffuse from the bulk liquid into the pores of the adsorbent (Dahri *et al*., 2014).

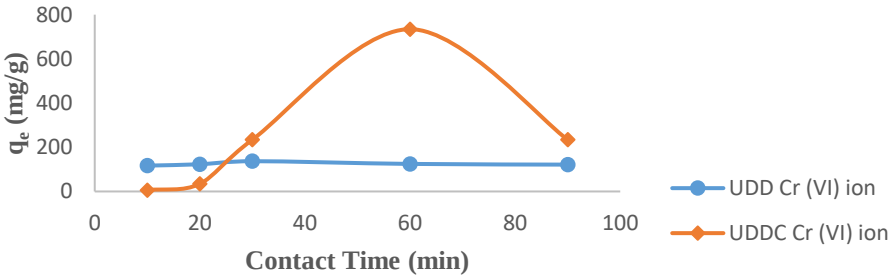

Figure 5: Effect of Contact Time for Cr (VI) ion onto UDD Peels & UDDC

Effect of pH

The pH of the solution has a significant effect on the uptake of metal ions since it determines the chemistry of the surface charge of the adsorbent and the degree of ionization as well as speciation of the adsorbate molecules

(Gupta *et al*., 2009; Boudaoud *et al*., 2017). The pH solution governing the targeted metal ion [Cr (VI)] ion onto UDD and UDDC is presented in Figure 6. It can be seen clearly from the results that; the metal ion was highly pH dependent. The adsorption capacity increased sharply when pH increased from 2 to 8 on the adsorbents under study. This adsorption behaviour could be explained based on surface charge and proton Cr (VI) ion adsorption. At a very low pH, the number of H_3O^+ ions exceed that of the metal ions several times and the surface is most likely covered with H_3O^+ ions, which account for less adsorption (Gupta and Bhattacharyya, 2008; Anna *et al*., 2015). When the pH increases, more H_3O^+ ions leave the adsorbent surface making the sites available to the metal ions, which increasingly bind to the adsorbent surface through a mechanism controlling electrostatic attraction (Jain *et al*., 2015; Nguyen *et al*., 2019).

Consequently, hexavalent chromium exists in a different forms of oxidation states and the stability of these forms depends upon the pH of the solution. At pH 1.0, the chromium ions exist in the form of (chromic acid) H_2CrO_4, while in the pH range 2-6 different forms of chromium ions such as $Cr_2O_7^-$, $HCrO_4^-$, CrO_{10}^{2-}, $Cr4O_{13}^{2-}$ coexist of which (hydrogen chromate) $HCrO_4^-$ predominates. As the pH increases this form shifts to CrO_4^{2-} (chromate) and CrO_7^{2-} (dichromate) (Labied *et al*., 2018; Sweetman *et al*., 2017).

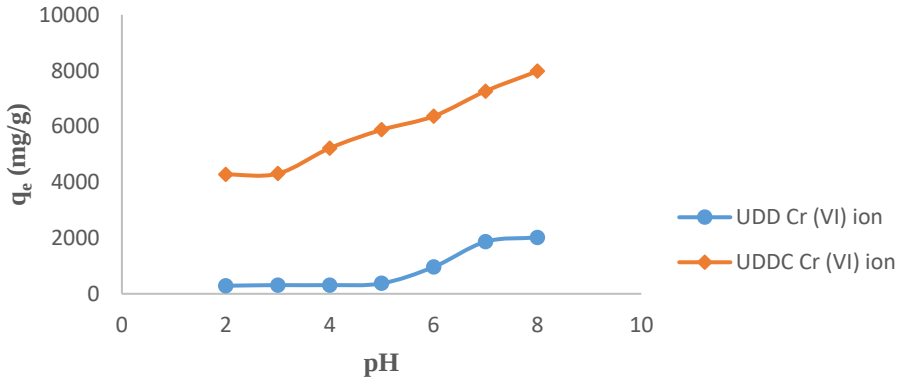

Figure 6: Effect of pH for Cr (VI) ion onto UDD Peels & UDDC

Effect of Temperature

Temperature is another significant adsorption parameter as it changes the adsorption limit of the adsorbent (Goharshadi and Moghaddam, 2015). The impact of temperature on the balance takes up of Cr (VI) ion onto UDD and UDDC are researched at different temperatures of 40-80 ºC as shown in Figure 7. Other adsorption conditions were kept constant. The maximum quantity adsorbed was achieved at (50 ºC and 80 ºC) onto UDD and UDDC respectively. The increase in the quantity adsorbed with increasing temperature may be attributed to the increasing accessibility of the adsorbent active sites and possibly chemical interactions between the surface functional groups of the adsorbent and the metal ions (Abdus-Salam and Buhari, 2014). Similarly, at a lower temperature, the kinetic energy of the metal ion was low; therefore, contact between the metal ion and the active sites of the adsorbents was insufficient leading to a decrease in adsorption capacity (Afkhami and Conway, 2002). The results obtained are in line with the literature reported on desert date seed shells by (Yunusa *et al*., 2020).

Generally speaking, increasing the temperature reduces the solution viscosity and thus, improved the ion's diffusion to attain the maximum adsorption, thereby, allowing the

enhancement of the adsorption performance. However, the effect of temperature in the adsorption process of metal ions from aqueous solution can be affected in two different ways depending on heat emitted or absorbed. The increasing temperature causes an increase in the adsorption rate for endothermic adsorption while causing a decrease in the adsorption rate for exothermic adsorption (Tahoon *et al.*, 2020).

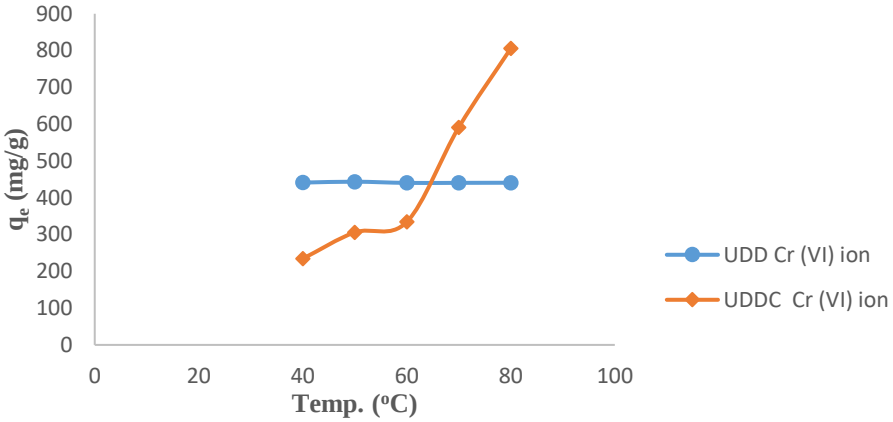

Figure 7: Effect of Temp. for Cr (VI) ion onto UDD Peels & UDDC

Adsorption Isotherm Models

The term Isotherm defines as the relationship between the equilibrium concentration and the amount of adsorbate adsorbed at a constant temperature. It can be described graphically how adsorbates interact with adsorbents using correlation coefficient (R^2) value to understand the conformity of the isotherm model applied to the experimental data (Dada *et al.*, 2016; Yunusa and Ibrahim, 2019). The linear plots of the Langmuir, Freundlich and Temkin isotherm models for the adsorption of Cr (VI) ion onto the UDD and UDDC are presented in Figures 8a & b to 10a & b respectively. The straight lines plot of the isotherms confirmed the satisfactory fits of the application of the Langmuir, Freundlich and Temkin isotherm models to the adsorption of Cr (VI) ion onto the UDD and UDDC.

Langmuir Isotherm

The Langmuir isotherm represents the equilibrium distribution of metal ions between the solid and liquid phases (Moosa *et al.*, 2015). The Langmuir isotherm is represented in eq. (3) (Chowdhury *et al.*, 2011)

$$q_e = \frac{q_m K_L C_e}{1 + K_L C_e} \quad (3)$$

Langmuir adsorption parameters were determined by transforming the Langmuir equ. (3) into the linear form as:

$$\frac{C_e}{q_e} = \frac{1}{q_m} + \frac{1}{q_m K_L} C_e \quad (4)$$

Where, C_e = the equilibrium concentration of adsorbate (mg/L) q_e = the amount of metal adsorbed per gram of the adsorbent at equilibrium (mg/g), q_m = maximum monolayer coverage capacity (mg/g) and K_L = Langmuir isotherm constant (mg/L).

The Langmuir parameters q_m and K_L are calculated from the slope and the intercept. It was observed from Table 2 that the adsorption data fitted best into the Langmuir isotherm model correlation coefficients (R^2) values close to unity for UDD and UDDC are 0.9069 and 0.969 respectively. Meanwhile, the correlation coefficient suggests that equilibrium data were described Langmuir isotherm model signifying a chemisorption adsorption (Hao *et al*., 2010). However, this observation was further supported by the closeness of experimental data [q_o 114.11 (mg/g)] and theoretical values [q_m 111.11 (mg/g)] for UDD while [q_o 741.14 (mg/g) [q_m 746.27 (mg/g)] for UDDC. The closeness between the experimental data and theoretical values could be attributed to the homogenous distribution of the active sites on the surface of the adsorbents and that the adsorption indicates good monolayer coverage in nature (Dada *et al*., 2016; Abdus-Salam and Ikudayisi, 2017).

Freundlich Isotherm

The Freundlich model, (1906) is perhaps the most widely used non-linear adsorption equilibrium model, which can be shown to be thermodynamically rigorous for adsorption on heterogeneous surfaces (Mansouriieh *et al*., 2016). These data often fit the empirical equation proposed by Freundlich:

$$q_e = K_f C_e^{\frac{1}{n}} \quad (5)$$

Where K_f= Freundlich isotherm constant (mg/g), C_e = the equilibrium concentration of adsorbate (mg/L), q_e= the amount of metal adsorbed per gram of the adsorbent at equilibrium (mg/g) and n = adsorption intensity. The logarithmic form of the equation (5) becomes:

$$\log q_e = \log K_f + \frac{1}{n} \log C_e \quad (6)$$

The constants are Freundlich's constant characteristics of the system. The Freundlich parameters are calculated from the slope and intercept (Dada *et al*., 2012). The summary Freundlich parameters of Cr (VI) ion onto UDD and UDDC are presented in Table 2. It can be observed clearly from Table 3.2 that UDDC fitted well into the Freundlich isotherm model with a correlation coefficient (R^2) value of 0.9406 close to unity, whereas, UDD correlation coefficient was far from unity with (R^2) 0.4873. The UDD does not fit into Freundlich isotherm which means that it is not multilayer in nature (Boudaoud *et al*., 2017). The Freundlich isotherm constants and n indicate adsorption capacity and intensity respectively. When the value of n lies between one and ten and is less than unity, they are said to be true reflections of favourable and normal adsorption (Ghasemi *et al*., 2014).

Temkin Isotherm

The Temkin adsorption isotherm contains a factor that considers the interaction between adsorbates. The model assumes that the heat of adsorption of all molecules in the layer will decrease linearly rather than logarithmically with coverage at average concentrations. The heat of adsorption is characterized by a uniform distribution of binding energies between adsorbent and adsorbate (Edet and Ifelebuegu, 2020). The model is given by the following equations:

$$q_e = \frac{RT}{b} \ln(A_T C_e) \quad (7)$$

$$q_e = \left(\frac{RT}{b}\right) \ln A_T + \left(\frac{RT}{b}\right) \ln c_e \quad (8)$$

$$B = \frac{RT}{b_T} \quad (9)$$

$$q_e = B \ln A_T + B \ln c_e \quad (10)$$

A_T = Temkin isotherm equilibrium binding constant (L/g), b_T = Temkin isotherm constant, R = universal gas constant (8.314 J/mol/K), T = Temperature at 298 K and B = Constant related to the heat of sorption (J/mol).

It was observed from Table 2 that the fitness of Temkin isotherm is achieved on UDDC Cr (VI) with (R^2) values 0.9637 while UDD did not fit well into the Temkin isotherm model. Apart from the information obtained from the correlation coefficient (R^2), Temkin isotherm also gives insight into the interaction between adsorbent and adsorbate from Temkin isotherm constant related to the heat of adsorption b_T (J/mol) which decreased as a result of surface coverage. Therefore, when the heat of adsorption b_T (J/mol) is less than 8 signifies that attractive forces are weak and physical in nature whereas values greater than 8 are indicative of strong and chemical interaction (Theivarasu and Mylsamy, 2010).

As reported in Table 2, the b_T (J/mol) results revealed that UDDC Cr (VI) with 5.02 J/mol shows weak and physical in nature while UDD established strong chemical interaction with 70.61 J/mol. The results obtained are in agreement with the b_T and R^2 values (52.36 J/mol and 0.917) reported by Azeez and Adekola, (2016).

Table 2: Summary Adsorption Isotherm Models of UDD and UDDC

Langmuir parameters	**UDD Cr (VI)**	**UDDC Cr (VI)**	**Freundlich parameter**	**UDD Cr (VI)**	**UDDC Cr (VI)**	**Temkin parameters**	**UDD Cr (VI)**	**UDDC Cr (VI)**
q_o (mg/g)	114.11	741.14	$\frac{1}{n}$	-1.07	-1.03	A_T (L/mg)	0.61	1.82×10^{-4}
q_m (mg/g)	111.11	746.27	N	-0.93	-0.97	b_T (J/mol)	70.61	5.02
K_L (L/mg)	1.79	2.06	K_f (mg/g)	0.222	0.425	B	35.088	493.23
R_L	5.58×10^{-04}	1.21×10^{-03}	R^2	0.4873	0.9406	R^2	0.2458	0.9637
R^2	0.9069	0.969						

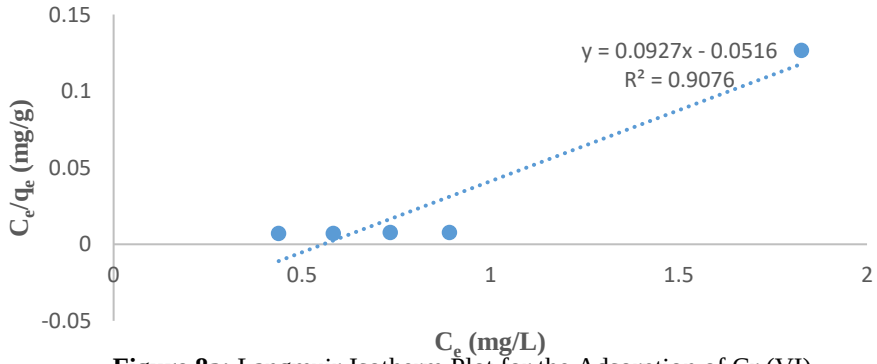

Figure 8a: Langmuir Isotherm Plot for the Adsorption of Cr (VI) ion onto UDD

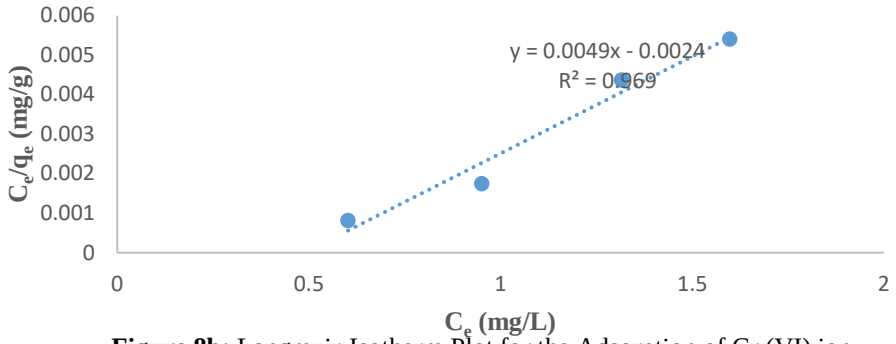

Figure 8b: Langmuir Isotherm Plot for the Adsorption of Cr (VI) ion onto UDDC

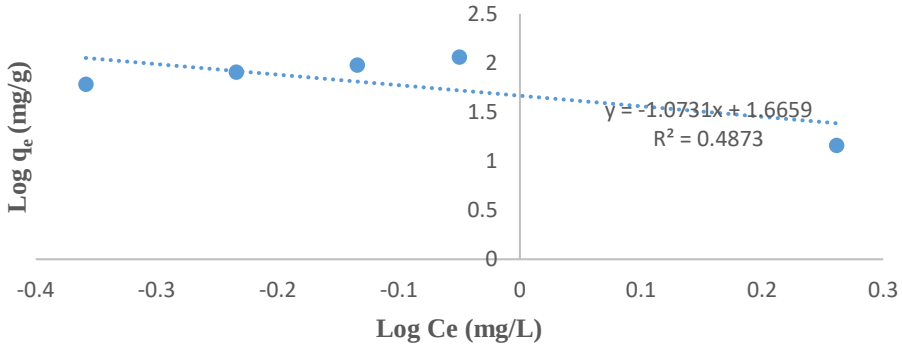

Figure 9a: Freundlich Isotherm Plot for the Adsorption of Cr (VI) ion onto UDD peel

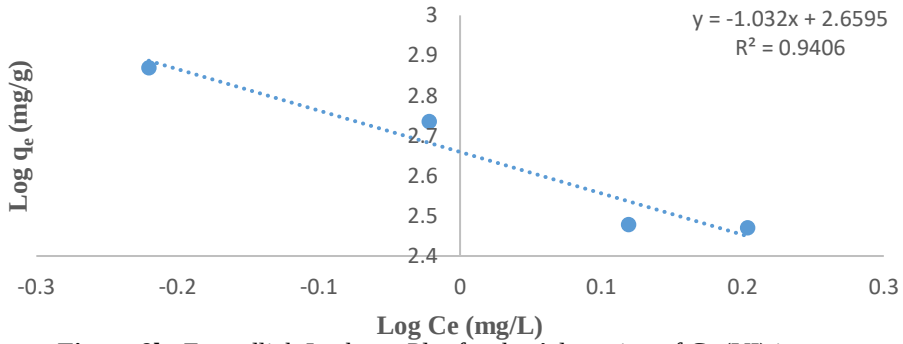

Figure 9b: Freundlich Isotherm Plot for the Adsorption of Cr (VI) ion onto UDDC

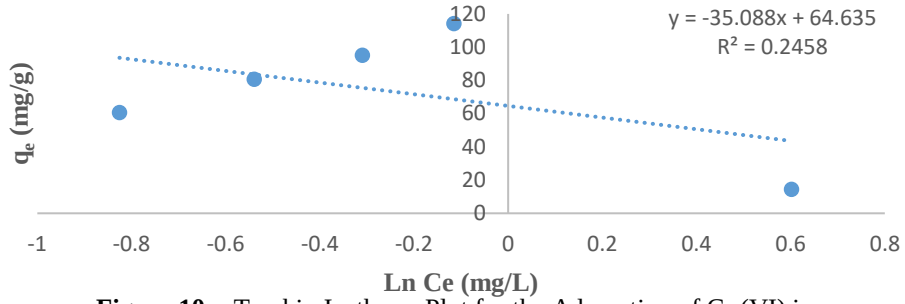

Figure 10a: Temkin Isotherm Plot for the Adsorption of Cr (VI) ion onto UDD peel

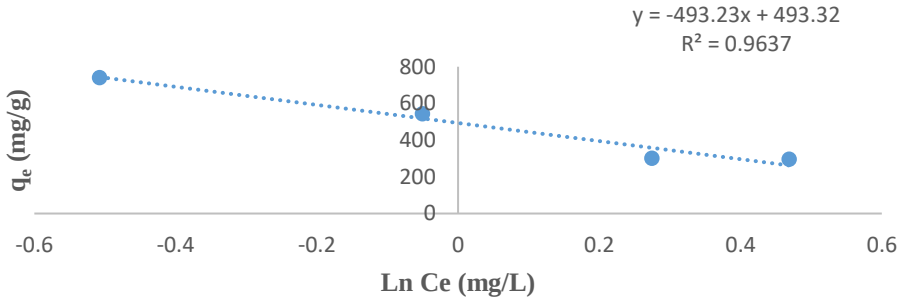

Figure 10b: Temkin Isotherm Plot for the Adsorption of Cr (VI) ion onto UDDC

Adsorption Kinetics Models

The adsorption kinetics provides the rate of adsorbate uptake onto the activated adsorbent within the equilibrium contact time (Danmallam *et al*., 2020). The Pseudo-first order, Pseudo-second order kinetic models and Intra-particle diffusion adsorption kinetic models were implemented to evaluate the rate constant of the adsorption process. The linearity of the plots with correlation coefficient values (R^2) that are very close to unity is an indication that the adsorption process followed any of the aforementioned kinetic models (Abdus-Salam and Buhari, 2014). The summary of the kinetic parameters for Pseudo-first order, second order and Intra-particle diffusion models are shown in Table 3 Cr (VI) ion onto UDD and UDDC respectively. The plots of Pseudo-first order, second order and Intra-particle diffusion models of the above-mentioned models are presented in Figures 11a & b – 13a & b respectively.

Pseudo-first order Kinetics

The linear form of the Pseudo-first order kinetic model described by Lagergren, (1898) is expressed by the following equation:

$$In\,(q_e - q_t) = In\,q_e - k_1 t \qquad (11)$$

where q_e *and* q_t are the values of the amount adsorbed per unit mass at equilibrium and at any time t. The values of k_1 can be obtained from the slope of the linear plot of $In\,(q_e - q_t)$ vs. t.

It was observed from Table 3 that both adsorbents poorly agree with the pseudo-first-order kinetic model on the fact that their correlation coefficient values (R^2) are far away from unity (0.6359 and 0.6073 respectively) and the disparity between the q_e experimental and q_e calculated. It could be concluded that the pseudo-first-order kinetic model is not the most suitable model to judge these adsorbents. This reason can be attributed to the fact that the pseudo-first-order model can only describe the adsorption kinetics of the initial stage and

cannot give an accurate description and information of the whole adsorption process (Wu *et al*., 2019; Yunusa *et al*., 2020). However, the q_e calculated differs significantly from the q_e experimental on both adsorbents tested on Cr (VI) ion. This could be related to the rate controlling the steps for the uptake of ions is resistance to the boundary layer (Akinyeye *et al*., 2020). These results were in agreement with the literature reported by Ghasemi *et al*. (2014)

Pseudo-second-order Kinetics

Generally speaking, the pseudo-second-order kinetic model is the rate-limiting step of chemisorption involving forces sharing or exchange of electrons between the adsorbate and the adsorbent (Akinyeye *et al*., 2020). The adsorption parameters derived from the pseudo-second-order kinetic model of Cr (VI) ion onto UDD and UDDC are summarized in Table 3.

The linear form as described by Ho and McKay, (1999) is represented by the following equation:

$$\frac{t}{q_t} = \frac{1}{\left(\frac{1}{k_e q_e^2}\right) + \left(\frac{1}{q_e}\right) \cdot t} \quad (12)$$

where k_2 is the second order rate coefficient (g/min/mg), q_e is the equilibrium amount of adsorbate adsorbed per unit mass of the adsorbent (mg/g), qt is the amount of adsorbate adsorbed per unit mass of adsorbent at time t (mg/g), and t is the time (min). The equilibrium adsorption capacity (q_e), and the constant k_2 can be obtained from the slope and intercept of a plot $\frac{t}{q_t}$ against t.

It can be seen from Table 3 that the degree of correlation coefficient (R^2) is found to be extremely high with 0.9173 and 0.9943 on UDD and UDDC tested. It could be concluded that both the adsorbents fitted perfectly well into the pseudo-second-order kinetic model because of the strong interaction between the adsorbent and the adsorbates (Adebayo *et al*., 2016). Meanwhile, the q_e calculated obtained from the pseudo-second-order model for the adsorption of UDD and UDDC are in conformity with the q_e experimental (q_{ecal} 114.11 mg/g) (q_{eexp} 111.11 mg/g) for UDD and (q_{ecal} 769.23 mg/g) (q_{eexp} 741.14 mg/g) for UDDC respectively. The results obtained are in agreement with the observation reported by Akinyeye *et al*. (2020); Dada *et al*. (2016).

Intra-particle Diffusion Kinetic

The intra-particle diffusion kinetic model assumes that solubilized metal ions transport from the aqueous medium to the adsorbent materials then an intra-particle diffusion assay takes place (Mohamed *et al*., 2019). The values of R^2 (correlation coefficient) are taken into consideration as a measure of the applicability and goodness of fit of the experimental data obtained from the slope of the plot q_t vs $t^{1/2}$. The intra-particle diffusion equation is given (Cheung *et al*., 2007):

$$q_t = k_i\, t^{1/2} + C \quad (13)$$

where q_t is the amount of solute on the surface of the sorbent at time t (mg/g) and k_i is the intraparticle diffusion rate constant (mg/g $min^{1/2}$).

The summary of the results obtained is presented in Table 3. It can be observed that the R^2 value of UDD is greater than that of UDDC (0.836 and 0.565) respectively. The bulk diffusion is the important aspect attributed to the initial linear portion meanwhile; equilibrium is represented by the plateau portion and intra-particle diffusion when it passes through the origin (Nwosu *et al*., 2019). Similarly, the rate constant of pore diffusion K_i values of UDD and UDDC is 0.0161 and

0.0072 ($mg/g/min^2$) respectively. The corporality of the linear relationship between amount q_e against $t^{1/2}$ signifies that intra-particle diffusion partakes during the adsorption process. If the straight line of the plot of q_e against $t^{1/2}$ went through the origin, then intra-particle diffusion becomes the controlling step. However, if the straight line does not pass through the origin, it indicates that the intra-particle diffusion is not the only controlling step but that boundary surface effects are also involved (Nwosu *et al*., 2017).

Table 3: Summary Kinetic Model Isotherms of UDD and UDDC

Pseudo-first order parameters	**UDD Cr (VI)**	**UDDC Cr (VI)**	**Pseudo-second order parameters**	**UDD Cr (VI)**	**UDDC Cr (VI)**	**Intra-particle parameters**	**UDD Cr (VI)**	**UDDC Cr (VI)**
K_1 (min^{-1})	0.0248	0.0271	K_2 (g/mg/min)	3.53×10^{-04}	1.43×10^{-05}	k_i ($mg/g/min^2$)	0.0161	0.0072
$q_{e\ exp}$ (mg/g)	114.11	741.14	$q_{e\ exp}$ (mg/g)	114.11	741.14	C	12.134	37.78
$q_{e\ cal}$ (mg/g)	1.257	0.607	$q_{e\ cal}$ (mg/g)	111.11	769.23	R^2	0.836	0.565
R^2	0.6359	0.6073	R^2	0.9173	0.9943			

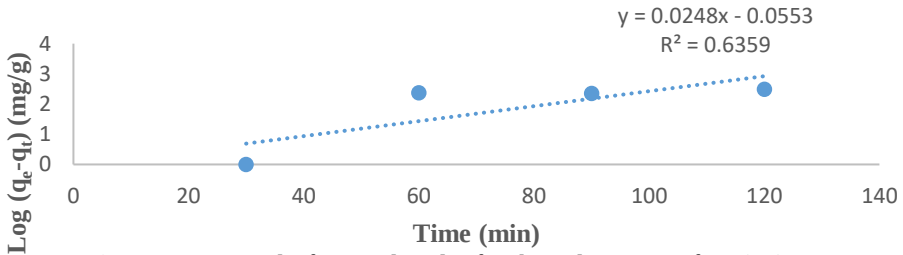

Figure 11a: Pseudo-first Order Plot for the Adsorption of Cr (VI) ion onto UDD peel

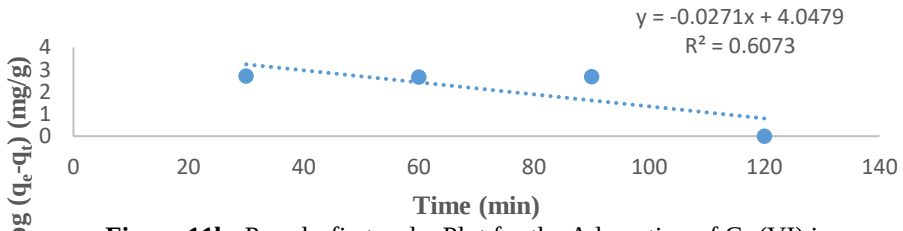

Figure 11b: Pseudo-first order Plot for the Adsorption of Cr (VI) ion onto UDDC

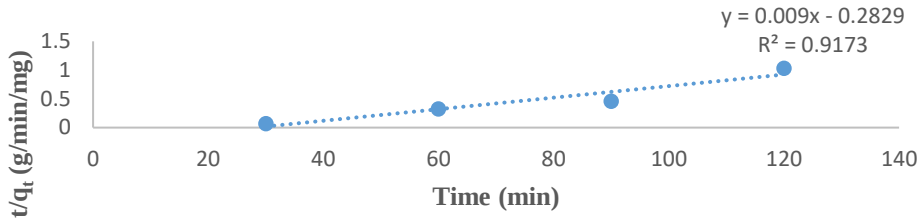

Figure 12a: Pseudo-second Order Plot for the Adsorption of Cr (VI) ion onto UDD peel

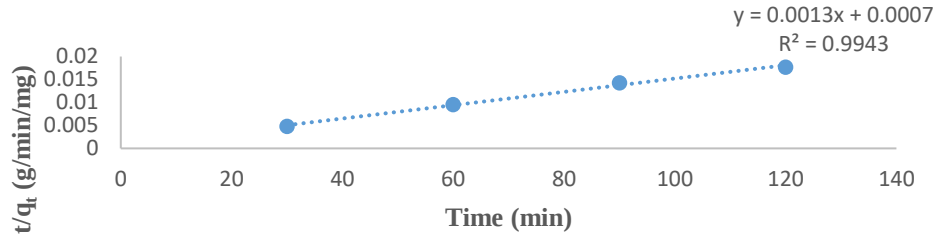

Figure 12b: Pseudo-second order Plot for the Adsorption of Cr (VI) ion onto UDDC

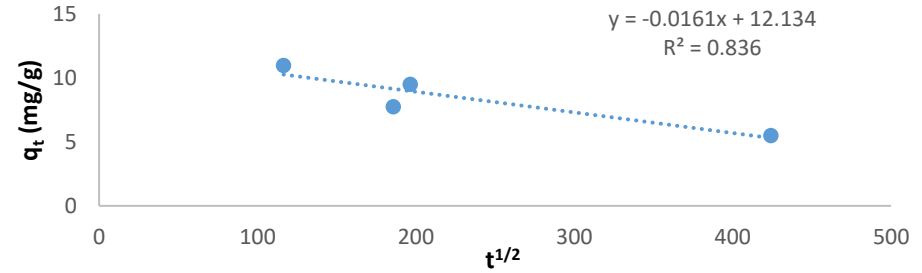

Figure 13a: Intra-particle diffusion Plot for the Adsorption of Cr (VI) ion onto UDD peel

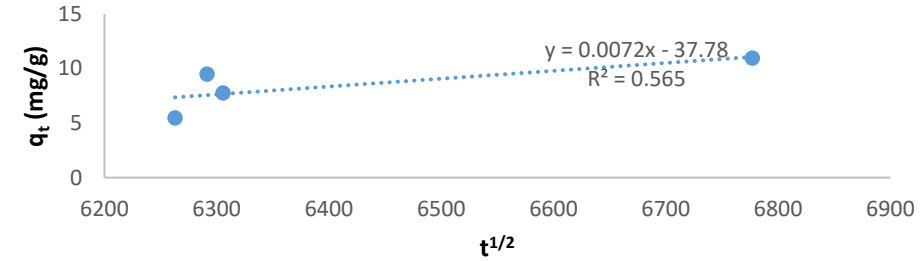

Figure 13b: Intra-particle diffusion Plot for the Adsorption of Cr (VI) ion onto UDDC

CONCLUSION

In this study, the adsorption of unmodified desert date peels composited with functionalized carbon nanotubes have been prepared, characterized and used for the adsorption of Cr (VI) ion by using batch experiment. The maximum adsorption capacity of Cr (VI) ion adsorbed on UDD and UDDC are found to be 114.11 mg/g and 741.14 mg/g. The adsorption capacity increased sharply when pH increased from 2 to 8 on the adsorbents under study. This adsorption behavior could be explained on the basis of surface charge and proton of Cr (VI) ion adsorption. The maximum quantity adsorbed was achieved at 80 ^{o}C onto UDD and UDDC respectively. The adsorption isotherm observed in the following trend; Temkin > Freundlich > Langmuir for UDDC. Meanwhile, pseudo-second-order kinetic isotherm fitted best for both UDD and UDDC respectively. The results revealed that UDD has the potentials to be used as alternative adsorbent particularly when composited with functionalized carbon nanotubes in remediation of Cr (VI) ion in wastewater.

ACKNOWLEDGMENTS

The authors really appreciate the efforts of Prof. N. Abdus-Salam Faculty Physical Sciences, Department of Chemistry, University of Ilorin, Nigeria for equipping his laboratory for core teaching and research work with all the necessary equipment where this research work was carried out successfully.

CONFLICTS OF INTEREST

The authors declare no conflict of interest.

REFERENCES

Abdus-Salam, N. and Buhari, M. (2014). Adsorption of Alizarin and Fluorescein Dyes on Adsorbent prepared from Mango Seed. *The Pacific Journal of Science and Technology, 15*: 232-235

Abdus-Salam, N. and Buhari, M. (2016). Adsorption of Alizarin and Fluorescein Dyes onto Palm Seeds Activated Carbon: Kinetic and Thermodynamic Studies. *Journal of the Chemical Society of Pakistan, 38*: 604-612

Abdus-Salam, N. and Bello, M. O. (2015). Kinetics, thermodynamics and competitive adsorption of lead and zinc ions onto termite mound. *International Journal of Environmental Science and Technology,* 12: 3417–3426

Abdus-Salam, N. and Ikudayisi, V. A. (2017). Preparation and characterization of synthesized goethite and goethite-date palm seeds charcoal composite. *Ife Journal of Science,* 19: 99-107

Adebayo, G. B., Adegoke, H. I. and Fauzeeyat, S. (2020). Adsorption of Cr(VI) ions onto goethite, activated carbon and their composite: kinetic and thermodynamic studies. *Applied Water Science,* 10: 13-18

Adebayo, G. B., Abdus-Salam, N. and Alimi, E. S. (2014). Adsorption of Lead (II) ions by Activated Carbon prepared from different parts of *Jatropha Curcas* Plant. Publication of faculty of science, Unilorin, *Ilorin Journal of Science, 1*: 28-49

Adegoke, H. I., Adekola, F. A. and Abdulraheem, M. N. (2016). Kinetic and thermodynamic studies on adsorption of sulphate from aqueous solution by magnetite, activated carbon and magnetite-activated carbon composites. *Nigerian Journal of Chemical Research, 22*: 39-65

Adegoke, I. A., Adekola, F. A., Fatoki, O. S. and Ximba, B. J. (2014). Adsorption of Cr (VI) on synthetic hematite (alpha-

Fe_2O_3) nanoparticles of different morphologies. *Korean Journal of Engineering, 31:* 142-152

Afkhami, A. and Conway, B. E. (2002). Investigation of removal of Cr (VI), Mo (VI), W (VI), V (IV), and V (V) oxy-ions from industrial waste-waters by adsorption and electrosorption at high-area carbon cloth. *Journal of Colloid Interface Science, 251:* 248–255

Agency for Toxic Substances and Disease Registry (ASTDR) (2020). Toxicological Profile Division of Toxicology and Human Health Sciences.

Agency for Toxic Substances and Disease Registry (ATSDR) (1998). Toxicological Profile for Chromium. U.S. Public Health Service, U.S. Department of Health and Human Services, Atlanta, GA

Aguilar, D. L. G., Miranda J. P. R., Muñoz, J. A. E. and Fredy, J. (2019). Betancur Coffee Pulp: *A Sustainable Alternative Removal of Cr (VI) in Wastewaters Processes, 7*: 403

Ahmed, A., Abdulhakim, S. A., Ishaq, K., Saka, A. A., Peter, M. S. and Chidinma, O. U. (2017). Carbon Nanotubes: Mechanism, Langmuir Hinshelwood Growth Kinetics and It Application for the Removal of Chromium (VI). *Journal of Membrane Science & Technology, 7*: 1-10

Akinyeye, O. J., Ibigbami, T. B., Odeja, O. O. and Sosanolu, O. M. (2020). Evaluation of kinetics and equilibrium studies of biosorption potentials of bamboo stem biomass for removal of Lead (II) and Cadmium (II) ions from aqueous solution. *African Journal of Pure and Applied Chemistry, 14*: 24-41

Alghamdi, A. A., Al-Odayni, A. B., Saeed, W. S., Al-Kahtani, A., Alharthi, F. A. and Aouak, T. (2019). Efficient adsorption of lead (II), from aqueous phase solutions using polypyrrole-based activated carbon. *Materials, 12:* 20-29

Aneyo, I. A., Doharty, F. V., Adebesin, O. A. and Hammed, M. O. (2016). Biodegradation of pollutants in wastewater from pharmaceutical, textile and local dye effluent in Lagos, Nigeria. *Journal of Health and Pollution, 6*: 34–42

Anna, B., Kleopas, M., Constantine, S., Anestis, F. and Maria, B. (2015). Adsorption of Cd (II), Cu (II), Ni (II) and Pb (II) onto natural bentonite: study in mono- and multi-metal systems. *Environmental Earth Science, 73*: 5435–5444

Ayeni, O. (2014). Assessment of heavy metals in wastewater obtained from an industrial area in Ibadan, Nigeria. *RMZ – Materials and the Geoenvironment, 61*: 19–24

Azeez, S. O. and Adekola, F. A. (2016). Sorption of 4-Nitroaniline on Activated Kaolinitic Clay and Jatropha curcas Activated Carbon in Aqueous Solution. *Pakistan Journal of Analytical and Environmental Chemistry, 17*: 105-145

Bansal, M., Singh, D. and Garg, V. K. (2009). A comparative study for the removal of hexavalent chromium from aqueous solution by agriculture wastes' carbons. *Journal of Hazardous Materials, 171*: 83–92

Bishnoi, N. R, Bajaj, M, Sharma N. (2004). Adsorption of Cr (VI) on activated rice husk carbon and activated alumina. *Bioresource Technology, 91*: 305–307

Boudaoud, A., Djedid, M., Benalia, M., Chifaa, A., Bouzar, N. and Elmsellem, H. (2017). Removal of Nickel (II) and Cadmium (II) ions from wastewater by Palm Fibers. *Scientific Study and Research Journal, 18:* 391-406

Buhari M., Maigari, A. U., Abubakar, U. A., Sani, M. M. and Maigari, A. U. (2020). Batch Adsorption of Safranin Dye from an Aqueous Solution of *Balanites aegyptiaca* Seed Coats. *Asian Journal of Physical and Chemical Sciences, 8*: 48-54

Çalımlı, M. H., Demirbaş, Ö., Aygün, A., Alma, M. H., Nas, M. S., Khan, A. and Şen, F. (2019). Equilibrium, kinetics and thermodynamics of bovine serum

albumin from carbon-based materials obtained from food wastes. *BioNanoScience, 9*: 692–701

Cheung, W. H., Szeto, Y. S. and McKay, G. (2007). Intra-particle diffusion processes during acid dye adsorption onto chitosan. *Bioresources Technology*, 98*:* 2897–2904

Chowdhury, Z. Z., Zain, S. M. and Rashid, A. K. (2011). Equilibrium Isotherm Modelling, Kinetics and Thermodynamics Study for Removal of Lead from Waste Water. *E-Journal of Chemistry,* 8: 333-339

Dada, A. O., Inyinbor, A. A., Idu, E. I., Bello, O. M., Oluyori, A. P., Adelani-Akande, T. A., Okunola, A. A. and Dada, O. (2018). Effect of operational parameters, characterization and antibacterial studies of green synthesis of silver nanoparticles using Tithonia diversifolia. *Peer Journal, 10*: 1-17

Dada, A. O., Latona, D. F., Ojediran, O. J. and Nath, O. O. (2016). Adsorption of Cu (II) onto Bamboo Supported Manganese (BS-Mn) Nanocomposite: Effect of Operational Parameters, Kinetic, Isotherms, and Thermodynamic Studies, *Journal Applied Science and Environmental Management, 20*: 409-422

Dada, A. O., Olalekan, A. P., Olatunya, A. M. and Dada, O. (2012). Langmuir, Freundlich, Temkin and Dubinin–Radushkevich Isotherms Studies of Equilibrium Sorption of Zn^{2+} Unto Phosphoric Acid Modified Rice Husk. *Journal of Applied Chemistry,* 3: 38-45

Dahri, M. K., Kooh, M. R. R. and Lim, L. B. L. (2014). Water Remediation Using Low Cost Adsorbent Walnut Shell for Removal of Malachite Green: Equilibrium, Kinetics, Thermodynamic and Regeneration Studies. *Journal of Environmental Chemical Engineering, 2*: 1434–1444

Danmallam, A. A., Dabature, W. L., Pindiga, N. Y., Magaji, B., Aboki, M. A. Ibrahim, D., Zanna, U. A. S. and Muktar, M. S. (2020). The Kinetics of the Adsorption Process of Cr (VI) in Aqueous Solution Using Neem Seed Husk (*Azadirachta indica*) Activated Carbon. *Physical Science International Journal, 24*: 1-13

Dargahi, A., Golestanifar, H., Darvishi, P., Karami, A., Hasan, S. H., Poormohammadi, A. and Behzadnia, A. (2016). An Investigation and Comparison of Removing Heavy Metals (Lead and Chromium) from Aqueous Solutions Using Magnesium Oxide Nanoparticles. *Pollution Journal of Environmental Studies, 25*: 557-562

Dehgani, M. H., Taher, M. M., Bajpai, A. K., Heibati, B., Tyagi, I., Asiff, M., Agarwal, S. and Gupta, V. K. (2015). Removal of noxious Cr (VI) ions using Single walled Carbon Nanotubes and Multi-walled Carbon Nanotubes. *Chemical Engineering Journal, 279*: 344-352

Deveci, H. and Kar, Y. (2013). Adsorption of hexavalent chromium from aqueous solutions by bio-chars obtained during biomass pyrolysis. *Journal of Industrial and Engineering Chemistry, 19*: 190–196

Duan, C. Fang, L., Yang, C., Chen, W., Cui, Y. and Li, S. (2018). Reveal the response of enzyme activities to heavy metals through in situ zymography. *Ecotoxicology and Environmental Safety, 156*: 106–115

Edet, U. A. and Ifelebuegu, A. O. (2020). Kinetics, Isotherms, and Thermodynamic Modeling of the Adsorption of Phosphates from Model Wastewater Using Recycled Brick Waste. *Processes, 8:* 1-15

El-Shafey, E. I. (2005). Behavior of reduction-sorption of chromium (VI) from an aqueous solution on a modified rice husk. *Water, Air, and Soil Pollution, 163*: 81–102

Eltayeb, N. and Khan, A. (2019). Design and preparation of a new and novel nanocomposite with CNTs and its sensor applications. *Journal of Materials Research and Technology, 8*: 2238–2246

Fan, L., Wang, X., Wan, W., Liu, Q., Cai, Q. and Wan, Y. (2019). Rice Straw/Sewage Sludge-Based Composite Activated Carbon: Its Some Basic Properties and Adsorption Effect for Cr (VI). *The 5th Annual International Conference on Material Engineering and Application, 484*: 1-6

Farghali, A. A., Bahgat, M., El Rouby, W. M. A. and Khedr, M. H. (2012). Decoration of MWCNTs with CoFe2O4 Nanoparticles for Methylene Blue Dye Adsorption. *Journal of Solution Chemistry, 41*: 2209–2225

Farghali, A. A., Tawab, H. A. A., Moaty, A. M. and Khaled, R. (2017). Functionalization of acidified multi-walled carbon nanotubes for removal of heavy metals in aqueous solutions. *Journal of Nanostructure Chemistry, 7:* 101–111

Freundlich, H. (1906). Adsorption in solutions. *Physical Chemistry*, 57: 385 –470

Gebretsadik, H., Gebrekidan, A. and Demlie, L. (2020). Removal of heavy metals from aqueous solutions using *Eucalyptus Camaldulensis*: An alternate low cost adsorbent. *Cogent Chemistry, 6*: 1-16

Ghasemi, M., Naushad, M., Ghasemi, N. and Khosravi-Fard, Y. (2014). Adsorption of Pb (II) from aqueous solution using new adsorbents prepared from agricultural waste: Adsorption isotherm and kinetic studies. *Journal of Industrial and Engineering Chemistry, 20:* 2193-2199

Giwa, S. O., Moses, J. S., Adeyi, A. A. and Giwa, A. (2019). Adsorption of Atrazine from Aqueous Solution Using Desert Date Seed Shell Activated Carbon. *ABUAD Journal of Engineering Research and Development, 1*: 317-325

Goharshadi, E. K. and Moghaddam, M. B. (2015). Adsorption of hexavalent chromium ions from aqueous solution by graphene nanosheets: kinetic and thermodynamic studies. *International Journal Environmental Science and Technology, 12:* 2153–2160

Gomez, V. and Callao, M. P. (2006). Chromium determination and speciation since 2000, *Trends in Analytical Chemistry, 25*: 10-15

Gupta, S. S. and Bhattacharyya, K. G. (2008). Immobilization of Pb (II), Cd (II) and Ni (II) ions on kaolinite and montmorillonite surfaces from aqueous medium. *Journal Environmental Management, 87:* 46–58

Gupta, V. K., Carrott, P. J. M., Ribeiro-Carrott, M. M. L. and Suhas, T. L. (2009). Low-cost adsorbents: growing approach to wastewater treatment. *Critical Review. Environmental Science Technology, 39*: 783–842

Habte, L., Shiferaw, N., Khan, M. D., Thriveni, T. and Ahn, J. W. (2020). Sorption of Cd^{2+} and Pb^{2+} on Aragonite Synthesized from Eggshell. *Sustainability, 12*: 1-15

Hao, Y. M., Chen, M. Hu, Z. B. (2010). Effective removal of Cu (II) ions from aqueous solution by amino functionalized magnetic nanoparticles, *Journal of Hazardous Materials, 184*: 392–399

Ho, Y.S. and McKay, G. (1999). Pseudo-Second-Order Model for Sorption Processes. *Process Biochemistry, 34*: 451-465

Jain, M., Garg, V. K., Garg, U. K., Kadirvelu, K. and Sillanpää, M. (2015). Cadmium Removal from Wastewater using Carbonaceous Adsorbents Prepared from Sunflower Waste. *International Journal of Environmental Resource*, 9: 1079-1088

Khan, A. A., and Khan, A. (2010). Ion-exchange studies on poly-o-anisidine Sn (IV) phosphate nanocomposite and its application as Cd (II) ion-selective membrane electrode. *Central European Journal of Chemistry, 8*: 396–408

Khan, A., Parwaz Khan, A., Khan, I., Oves, M., Khan, S., Asiri, A. and Facchetti, A. (2019). Facial synthesis of highly active polymer vanadium molybdate nanocomposite: Improved

thermoelectric and antimicrobial studies. *Journal of Physics and Chemistry of Solids, 13:* 148–155

Kim, M., Lee, J., Roh, H., Kim, D., Byeon, J. and Park, J. (2017). Effects of Covalent Functionalization of MWCNTs on the Thermal Properties and Non-Isothermal Crystallization Behaviours of PPS Composites. *Journal of Polymer Research, 9*: 1-15

Kinuthia, G. K., Ngure, V., Beti, D. Lugalia, R., Wangila, A. and Kamau, L. (2020). Levels of heavy metals in wastewater and soil samples from open drainage channels in Nairobi, Kenya. *Community health implication Scientific Reports, 10*: 1-13

Kobya, M (2004). Removal of Cr (VI) from aqueous solutions by adsorption onto hazelnut shell activated carbon: Kinetic and equilibrium studies. *Bioresource Technology, 91:* 317–321

Krishna-Kumar, A. S., Jiang, S. J. and Tseng, W. L. (2015). Effective adsorption of chromium (VI)/Cr (III) from aqueous solution using ionic liquid functionalized multiwalled carbon nanotubes as a supersorbent. *Journal of Material Chemistry, 3*: 7044–7057

Labied, R., Benturki, O., Hamitouche, A. E. and Donnot, A. (2018). Adsorption of hexavalent chromium by activated carbon obtained from a waste lignocellulosic material (Ziziphus jujuba cores): Kinetic, equilibrium, and thermodynamic study. *Adsorption Science & Technology, 36*: 1066–1099

Langergren, S. (1898). About the Theory of so-called Adsorption of Soluble Substances. Band. 24(4): 1-39

Lee, X. J., Hiew, B. Y. Z., Lee, L.Y, Gan, S., Gopakumar, S.T (2017). Evaluation of The Effectiveness of Low-Cost Adsorbents from Oil Palm Wastes for Wastewater Treatment. *Chemical Engineering Transactions,* 56

Li, C., Tang, Y., Yao, K., Zhou, F., Ma, Q., Lin, H., Tao, M., Liang, J. (2006). Decoration of multiwall nanotubes with cadmium sulfide nanoparticles. *Carbon 44*: 2021–2026

Makeswari, M. and Santhi, T. (2013). Optimization of preparation of activated carbon from Ricinus communis Leaves by microwave-assisted Zinc Chloride chemical activation: Competitive Adsorption of Ni^{2+} ions from aqueous solution. *Journal of Chemistry, 10*: 1-12

Mansouriieh, N., Sohrabi, M. R. and Khosravi, M. (2016). Adsorption kinetics and thermodynamics of organophosphorus profenofos pesticide onto Fe/Ni bimetallic nanoparticles. *International Journal of Environmental Science and Technology, 13*: 1393–1404

Mohamed, H. S. Soliman, N. K., Abdelrheem, D. A., Ramadan, A. A., Elghandour, A. H. and Ahmed, S. A. (2019). Adsorption of Cd^{2+} and Cr^{3+} ions from aqueous solutions by using residue Podina gymnospora waste as promising low-cost adsorbent, *Heliyon, 5*: 1-16

Moosa, A. A., Ridha, A. M. and Abdullha, I. N. (2015). Chromium ions Removal from Wastewater using Carbon Nanotubes. *International Journal of Innovative Research in Science, Engineering and Technology, 4*: 275-282

Nguyen, K. M., Nguyen, B. Q., Nguyen, H. T. and Nguyen, T. H. H. (2019). Adsorption of Arsenic and Heavy Metals from Solutions by Unmodified Iron-Ore Sludge. *Applied Science Journal, 9*: 1-14

Nwosu, F. O., Adekola, F. A. and Salami, A. O. (2017). Adsorption of 4-Nitrophenol Using Pilli Nut Shell Active Carbon. *Pakistan Journal of Analytical and Environmental Chemistry, 18*: 69–83

Nwosu, F. O., Ajala, O. J., Okeola, F. O., Adebayo, S. A., Olankun, O. K. and Eletta, A. O. (2019). Adsorption of chlorotriazine herbicide onto unmodified and modified kaolinite: Equilibrium, kinetic and thermodynamic studies. *Egyptian Journal of Aquatic Research, 45:* 99-107

Peng, X., Chen, J., Misewich, J. A., Wong, S. S. (2009). Carbon nanotube

nanocrystal heterostructures. *Chemical Society Revision, 38:* 1076–1098

Sweetman, M. J., May, S., Mebberson, N., Pendleton, P., Vasilev, K., Plush, S. E. and Hayball, J. D. (2017). Activated Carbon, Carbon Nanotubes and Graphene: Materials and Composites for Advanced Water Purification. *Journal of Carbon Research, 3*: 1-29

Tahoon, M. A., Siddeeg, S. M., Alsaiari, N. S., Mnif, W. and Rebah, F. B. (2020). Effective Heavy Metals Removal from Water Using Nanomaterials: A Review. *Processes, 8*: 1-24

Thievarasu, C. and Mylsamy, S. (2010). Equilibrium and kinetic adsorption studies of Rhodamine-B from aqueous solution using cocoa (*Theobroma cocoa*) shell as a new adsorbent. *International Journal of Engineering Science Technology, 2*: 6284-6292

Ugbe, F. A. and Ikudayisi, V. A. (2017). The kinetics of eosin yellow removal from aqueous solution using pineapple peels. *Edorium Journal of Waste Management, 2*: 5–11

Vukovic, G. D. and Marinkovic, A. D. (2011). Removal of Cadmium from aqueous solutions by oxidized and ethylenediamine functionalized multi-walled carbon nanotubes. *Chemical Engineering Journal, 15*: 238-248

W.H.O. (2011). Guidelines for Drinking Water Quality (4th ed). WHO Press, Geneva, Switzerland

Wu, H., Chen, R., Du, H., Zhang, J., Shi, L., Qin, Y., Yue, L. and Wang, J. (2019). Synthesis of Activated Carbon from Peanut Shell as Dye adsorbent for Wastewater Treatment. *Adsorption Science and Technology, 37*: 34-48

Yang, J, Yu, M. and Chen, W. (2015). Adsorption of hexavalent chromium from aqueous solution by activated carbon prepared from Longan seed: Kinetics, equilibrium and thermodynamics. *Journal of Industrial and Engineering Chemistry, 21*: 414–422

Yudianti, R., Onggo, H., Saito, Y., Iwata, T. and Azuma, J. (2011). Analysis of Functional Group Sited on Multi-Wall Carbon Nanotube Surface. *The open materials science journal, 5:* 242-247

Yunusa, U., Usman, B. and Ibrahim, M. B. (2020). Kinetic and thermodynamic studies of malachite green adsorption using activated carbon prepared from desert date seed shell. *Algerian Journal of Engineering and Technology, 2*: 1-10

Yunusa, U. and Ibrahim, M. B. (2019). Reclamation of Malachite Green-Bearing Wastewater Using Desert Date Seed Shell: Adsorption Isotherms, Desorption and Reusability Studies. *ChemSearch Journal, 2*: 112 – 122

Zhang, J., Li, Y., Zhang, C. and Jing, Y. (2008). Adsorption of malachite green from aqueous solution onto carbon prepared from Arundo donax root. *Journal of Hazardous Materials,* 150: 774-782